COALESCENCE OF Au NANOPARTICLES: AN *IN-SITU Cs*-CORRECTED STEM STUDY AT LOW VOLTAGE.

R. Esparza[a*], C. Gutiérrez-Wing[b], R. Pérez[c] and M. José-Yacamán[d]

[a] Centro de Física Aplicada y Tecnología Avanzada, Universidad Nacional Autónoma de México, Boulevard Juriquilla 3001, Santiago de Querétaro, Qro. 76230, México.
[b] Instituto Nacional de Investigaciones Nucleares, Ciencias Aplicadas-Tecnología de Materiales, Carr. México-Toluca S/N, La Marquesa Ocoyoacac, Edo. de México 52750, México.
[c] Instituto de Ciencias Físicas, Universidad Nacional Autónoma de México (UNAM), Av. Universidad s/n, Cuernavaca, Mor., 62210, México.
[d] Department of Physics and Astronomy, The University of Texas at San Antonio, One UTSA Circle, San Antonio, TX 78249, USA.

*Corresponding author, E-mail: resparza@fata.unam.mx, phone: +52 442-192-6128 ext. 136

ABSTRACT
Nowadays, the characterization of many materials using transmission electron microscopy at low voltage is very attractive. In this work, we present set of images with atomic-level resolution of the in-situ coalescence phenomenon of gold nanoparticles using a spherical aberration-corrected scanning transmission electron microscopy (STEM) at 80 kV acceleration voltage. High-angle annular dark-field (HAADF)-STEM images with an atomic resolution was successfully obtained. HAADF-STEM images show the coalescence evolution of the gold nanoparticles, where some interesting image contrast characteristics were observed. The main mechanism of the coalescence phenomenon is the surface diffusion, where the twin boundaries of the nanoparticles act as barrier to the deformation. Molecular dynamics study of the coalescence of the Au nanoparticles at low temperature has been carried out. Molecular dynamical simulation of the coalescence phenomenon predicts rotations and surface diffusion of the nanoparticles. Simulated HAADF-STEM images of the coalescence evolution were obtained. Good agreement between simulation and experimental images was found.

Keywords: Electron-microscopy; spherical aberration-corrected; nanoparticles; coalescence-evolution; molecular-simulation.

COALESCENCIA DE NANOPARTÍCULAS DE Au: UN ESTUDIO *IN SITU* DE STEM CON CORRECCIÓN DE *Cs* A BAJO VOLTAJE.

RESUMEN
En la actualidad, la caracterización de muchos materiales mediante microscopía electrónica de transmisión utilizando bajos voltajes es muy atractiva. En este trabajo, se presenta una serie de imágenes con resolución atómica del fenómeno de coalescencia in situ de nanopartículas de oro utilizando microscopía electrónica de transmisión y barrido (STEM) con corrección de aberración esférica a un voltaje de aceleración de 80 kV. Se obtuvieron con éxito imágenes con resolución atómica en modo de campo oscuro anular de gran ángulo (HAADF). Las imágenes HAADF-STEM muestran la evolución de la coalescencia de las nanopartículas de oro, donde se observaron algunas características interesantes del contraste de la imagen. El mecanismo principal del fenómeno de coalescencia es la difusión de la superficie, donde las maclas de las nanopartículas actúan como barrera para la deformación. Estudios de dinámica molecular de la coalescencia de las nanopartículas de Au a baja temperatura fueron realizados. La simulación por dinámica molecular del fenómeno de coalescencia predice rotaciones y difusión superficial de las nanopartículas. Se obtuvieron imágenes simuladas de HAADF-STEM de la evolución de la coalescencia. Se encontró que las imágenes simuladas coinciden bien con las imágenes experimentales.

Palabras claves: Microscopía electrónica; aberración esférica corregida; nanopartículas; coalescencia; simulación molecular.

INTRODUCTION

Metallic nanoparticles have characteristic chemical and physical properties which usually are very different to the bulk material properties. The new properties are mainly induced by the quantum effects at extremely small sizes and also at the high values of surface to volume ratios [1]. The range of applications of the metallic nanoparticles includes energy, catalytic, magnetic, electronic and biomedical areas [2, 3]. The stability of nanoparticles is important for most of these applications [4]. However, these small particles tend to aggregate irreversibly during preparation or applications [5]. When two nanoparticles are in contact, they will coalesce in order to reduce their surface energy. This has been widely observed in transmission electron microscope experiments and also in molecular dynamic simulations [6-9]. Under these conditions the particles will tend to form a neck followed by a slower neck growth [10, 11]. Below the melting temperature, surface diffusion is the dominant mass transport mechanism for the coalescence of nanoparticles and therefore surface processes will control this process.

The coalescence of the particles into a single crystal will be driven by the reduction of the free energy with the generation of local free-energy minima stages with adjacent high barriers. Theoretical simulations based on molecular dynamic predict a lattice reorientation before this process begins. Furthermore, not all simulated particle pairs can find an adequate orientation for this phenomenon to occur. Experimental and theoretical results on the coalescence of nanoparticles demonstrate the importance of the crystallographic orientation on this behavior [12]. Thus, for example, hot-stage transmission electron microscopy studies on films consisting of indium tin oxide nanoparticles clearly show rotations of neighboring particles preceding their coalescence [12]. Both rotation and coalescence are observed well below half the melting temperature. Thus, theoretically as well as experimentally nanoparticle coalescence has shown to be a two-step process: first a reorientation of adjacent nanoparticles, and second their complete or incomplete coalescence depending on the matching of the crystallographic orientations.

There are recent reports which indicate that the electron beam in transmission or scanning electron microscopes can induce the coalescence of adjacent nanoparticles [13]. As mentioned before, the predominant nanoparticle transport phenomenon is the surface diffusion. The understanding of the influence of the electron beam on the coalescence process required a quantification of the atom's diffusion; therefore, *in-situ* studies of the coalescence phenomenon in the high-resolution (aberration-corrected) scanning transmission electron microscopy (STEM) can provide an important insight on the nature of this phenomenon. Some studies have evidenced the coalescence phenomenon using aberration-corrected STEM [6, 7, 14], however, these studies have been performed using STEM operating at high-voltage. In the past, the use of transmission electron microscopy (TEM) using high-voltages were favored because under these operating conditions the spherical (*Cs*) and chromatic (*Cc*) aberration effects are reduced, however, the development of Cs-correctors has allowed atomic resolution at lower operating voltages [15]. Currently, low-voltage STEM is of great interest because it produces less damage during observations mainly on electron-sensitive materials. The incorporation of aberration correctors, in particular the successful adoption of *Cs*-corrector in the STEM column, has allowed the increment in resolution up to the sub-Angstrom levels [16, 17].

In this work, we show the *in-situ* studies of the coalescence evolution with low-voltage STEM (80 kV) showing atomic resolution of gold nanoparticles. Simultaneously, the coalescence evolution was followed with molecular dynamical simulations, which provide the atomic structural models of the nanoparticle's coalescence at different times. These structural models were used for the

electron diffraction calculations of the STEM images which are finally compared with the experimental STEM images.

MATERIALS AND METHODS

Synthesis

Following the method reported first by Brust [18], gold nanoparticles passivated by 1-dodecanethiol were synthesized. All chemicals were purchased from Aldrich and used without any further purification.

At room temperature, an aqueous solution of hydrogen tetrachloroaurate trihydrate ($HAuCl_4 \cdot 3H_2O$) (2 ml, 0.1 M) was mixed under vigorous stirring with tetraoctylammonium bromide (TEAB) (1.0 mmol) dissolved in toluene (20 ml). After one hour, 1-dodecanethiol (0.3 ml) and an aqueous solution of sodium borohydride ($NaBH_4$) (6 ml, 0.4 M) were added. After 3 hours, the final product was obtained as a dark brown solid by precipitation in ethanol from the organic phase.

Characterization

The samples were analyzed using aberration-corrected scanning transmission electron microscopy (*Cs*-STEM) with a Jeol ARM200F FEG-STEM/TEM microscope operated at 80 kV and equipped with a CEOS *Cs*-corrector on the illumination system, which reaches a point-to-point resolution less than 0.1 nm. High-angle annular dark-field (HAADF)-STEM images were registered using a camera length of 80 mm, condenser lens aperture size of 40 microns and a collection angle of 50-180 mrad. The images were processed and filtered using the Richardson-Lucy/Maximum Entropy algorithm [19] for reduces the noise of the images recorded.

HAADF-STEM image simulations have been performed using the QSTEM software package [20] which uses the multislice algorithm [21]. Table 1 shows the parameters considered for the simulation corresponding to the experimental conditions of the microscope. It is important to observe the acceleration voltage (80 kV) and the obtained spherical aberration (743.1 nm) of the microscope operating conditions.

Table 1. Experimental parameters used for the STEM image simulations.

PARAMETER	**VALUE**
Acceleration voltage	80 kV
Defocus C_1	-2.503 nm
Coma B_2	39.93 nm
Threefold astigmatism A_2	77.01 nm
Spherical aberration C_3	743.1 nm
Star aberration S_3	67.29 nm
Fourfold astigmatism A_3	1.506 µm
Coma 5th order B_4	22.23 µm
Fivefold astigmatism A_4	15.45 µm
Spherical aberration 5th order C_5	-185.1 µm

Molecular Dynamics

Molecular dynamics (MD) simulations were used to model the coalescence processes of the Au nanoparticles. In order to simulate the coalescence processes of heteroclusters, the semiempirical analytic embedded-atom method (EAM) is used as the interatomic potential and the analytical methods of the homoclusters coalescence are extended to those of the heteroclusters [22]. The initial cuboctahedral structure was the approximate model of the nanoparticles identified during the *in-situ* STEM observations. The coalescent system studied consists of two nanoparticles with 490 and 990 atoms. One of the included cuboctahedral nanoparticles (990 atoms) has the double-twin atomic structures inside of the nanoparticle. In the initial configuration, the nanoparticles are facing off across the {111} faces. The simulation was performed based on the canonical ensemble (NVT) using the XenoView program [23].

RESULTS AND DISCUSSION

Studies at low-voltage scanning transmission electron microscopy (STEM) are very important to analyze many types of materials, mainly electron-sensitive materials. Nowadays, high-resolution images at low-voltage STEM are possible thanks to the incorporation of the spherical aberration (*Cs*) correctors [24, 25]. Figure 1a shows a low-magnification high-angle annular dark-field (HAAD)-STEM image obtained at 80 kV. As can be observed, the nanoparticles have a homogenous distribution with an average particle size of 3.6 nm (inset plot). As mentioned above, obtained high-resolution STEM images at low voltages are important because of their possible applications. Figure 1b shows a typical high-resolution HAADF-STEM image of Au nanoparticle. This nanoparticle has a face-centered cubic (fcc) structure and from the image and the fast Fourier transform (FFT) (figure 1c) d-spacings of 0.2377, 0.2363, 0.204 and 0.1428 nm were obtained. Such d-spacings correspond to (111), (1-11), (200) and (202) lattice planes respectively, and the nanoparticle is oriented at long [-101] zone axis. The most common structure found in this sample was fcc cuboctahedral, also some icosahedral structures were identified. The average particle size of the icosahedral nanoparticles was about 2 nm.

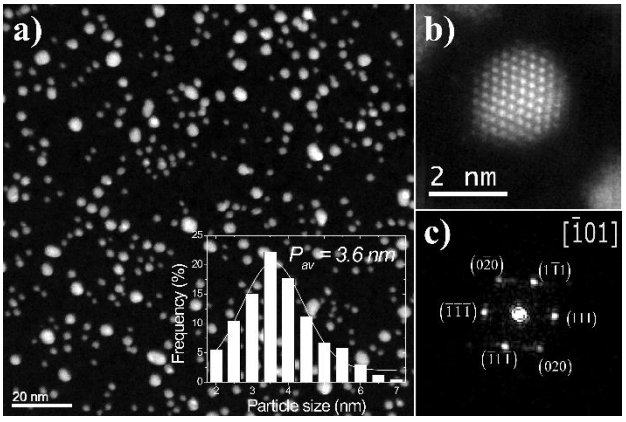

Fig. 1. a) Low magnification HAADF-STEM image of the Au nanoparticles with its particle size distribution, fb) HAADF-STEM image of Au nanoparticle with a fcc structure, and c) FFT of the Au nanoparticle.

Before starting the description of the coalescence evolution of the Au nanoparticles; it is necessary to analyze the structure of the involved nanoparticles in the process. Figure 2a shows the high-resolution HAADF-STEM image of some Au nanoparticles, where the image resolution is remarkable. As can be observed in this figure, the particle size of the nanoparticles A and B is 3.9 and 3.5 nm, respectively. The particle sizes are almost similar, thus effects related with the particle size can be discarded [10], where large deformations in the smaller particles have been observed. The particle A has an fcc structure and shows two [111] twin boundaries across the bulk of the specimen (TB1 and TB2). The formation of twin faults, where the twin plane represents a boundary between the twinned sub-units situated in mirror symmetry to each other, is characteristic for these types of nanoparticles. These twins may form via nucleation or as result of erroneously attaching atoms to the particle lattice during growth [26]. The crystallographic orientation of the nanoparticle A is close to [0-11] zone axis (figure 2b) and d-spacings 0.2337, 0.2324 and 0.2094 nm were measured. Such d-spacings correspond to (111), (-111) and (200) lattice planes respectively. The nanoparticle B seems to have a deformed fcc structure where its zone axis is close of [001] orientation (figure 2c); however, both the orientation and the structure are not clear; this may be related to the substrate surface, where the supported carbon membrane is not flat, also that the particles are surrounded manly by alkanethiol molecules.

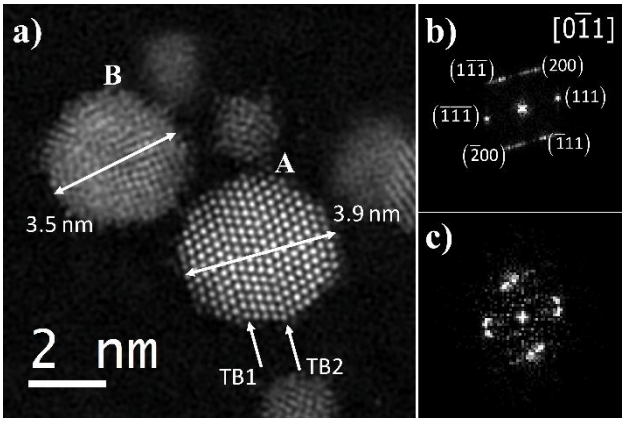

Fig. 2. a) HAADF-STEM image of two Au nanoparticles before the coalescence, b) and c) FFT's of the corresponding Au nanoparticles.

Figure 3 shows the initial stages of the coalescence evolution of the two Au nanoparticles in study. This phenomenon is illustrated with a series of aberration-corrected high-resolution HAADF-STEM images. Initially (figure 3a) the two small Au particles are oriented along different directions and the particle size is almost similar, as previously commented above. Thus, for example, the particle A has an fcc structure and it is oriented along a zone axis close to the [0-11] direction and the {111} atomic planes are clearly displayed. On the other hand, the adjacent nanoparticle B seems to have a deformed fcc structure. Figure 3b shows the first stage of the coalescence process. In this case, the main mechanism of the Au nanoparticles coalescence is the surface diffusion. However, only the atoms located on the surface of the [111] atomic planes close to the TB1 are moved through this diffusion mechanism; the trajectories of individual atoms can be identified as shown in this figure. From this analysis, the first surface diffusion of atoms from the particle A to B has been strongly evidenced, which can be seen as monatomic steps and that play a crucial role in diffusion processes [27]. Figure 3c clearly shows the first approach of the {111} atomic planes (shown with arrows). This important feature about the surface defects on the Au nanoparticle is notable, and the monatomic steps present on the nanoparticle are of the type (111) × (100) [28]; this behavior is due to the displacements of the outermost atomic layer, which cause an extension of the interplanar spacings (see upper arrow). At this moment, the particle B has not changed either the size or the orientation. It is important to mention that only the atoms close to the TB1 from the particle A are those that interact with the particle B. Figure 3d shows the initial formation of the sintering neck between the two nanoparticles (shown with a circle) were more atoms of particle A interact with particle B, besides the atoms on the contacting plane. A considerable amount of single Au atoms can be seen close to the other surfaces of the nanoparticle due to Ostwald ripening effects with neighbor small aggregates [7], which in this particular case does not affect the coalescence process. The growing of the sintering neck is mainly induced by the surface diffusion mechanism. After the formation of the sintering neck region between the coalescent nanoparticles, through the construction of low energy {111} atomic planes, the smallest coalescent particle (particle B) begins to rotate in the direction of the [0-11] zone axis (figures 3e and f). The atomic columns of one cuboctahedral can clearly be seen. In all the cases, the TB1 and TB2 always have the same size; the twin boundaries do not experience deformation. The crystalline units situated between the TB1 and TB2, and close to the TB2 are not deformed, only the crystalline unit situated close to the TB1. This indicates that TB1 act as a barrier to the deformation o coalescence. Now, it is important to mention that the beginning of this process up to this stage, was carried out over a period about of 1:10 minutes, which is a relatively short time since the contribution electron beam energy is very low.

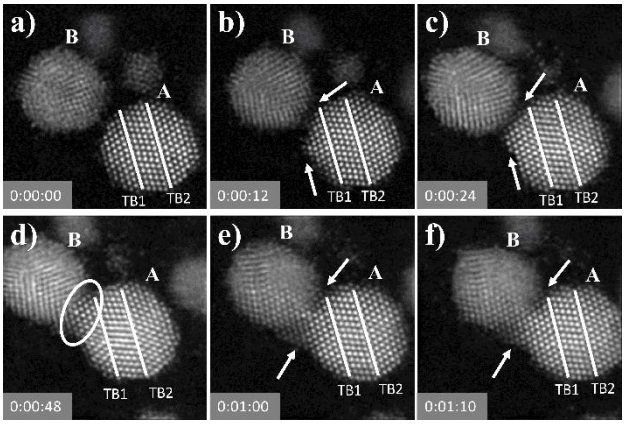

Fig. 3. a) - f) High resolution HAADF-STEM images of the coalescence of gold nanoparticles (the beginning of the process). Time of the process is indicated on the inset (h:m:s).

Figure 4 shows the HAADF-STEM sequence images indicating the last stages of the coalescence process. The rotation of the particle B continues to reach the orientation of the particle A (figure 4a), simultaneously with the continuous growth of the sintering neck region. Both particles start rotating and continue sintering to form a single nanoparticle or metastable nanoparticle. In figure 4b, the image contrast produced by the twin boundaries completely disappears. The rotation of the coalescent nanoparticle (particle B) has reached an orientation where the image contrast corresponding to the twin boundaries disappears and it seems as if it were a nanoparticle without defects. This can be described in terms of coincidence site lattices (CSL). Coincidence lattice model is deduced by considering two identical interpenetrating lattices. If one lattice is rotated through a common lattice point, for certain angles, site lattices come into coincidence, forming the so-called coincidence lattice [29]. These rotations are caused by small changes in the center of gravity of the coalescent nanoparticle that, together with the weak adhesion to the substrate, lead to orientation changes [9]. Figures 4c and 4d show the images of the rotated nanoparticle which reached an orientation close to [110]. The coalescent nanoparticle has the enough time to achieve this orientation, about 5 minutes. Further rotations of the coalescent nanoparticle reach crystalline orientations where the twin boundaries are visible again (figure 4e). The image contrast in this image confirms the evidence of the rotation of the coalescent nanoparticle. Finally, the last HAADF-STEM image of this set (figure 4f) shows the coalescent nanoparticle oriented along [110] zone axis, where the twin boundary image contrast is completely eliminated.

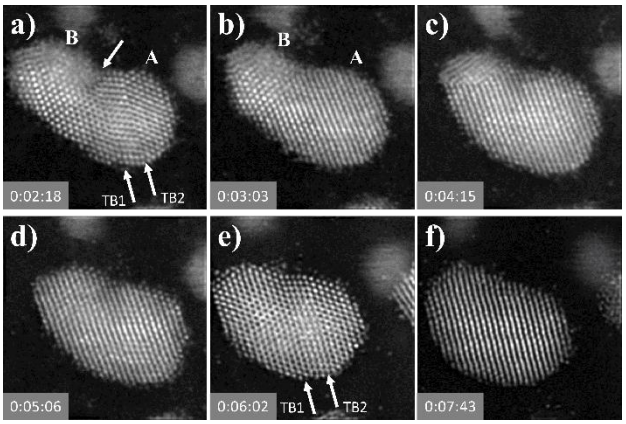

Fig. 4. a) - f) High resolution HAADF-STEM images of the coalescence of gold nanoparticles (the last stages of process). Time of the process is indicated on the inset (h:m:s).

The stages of coalescing nanoparticles computed by molecular dynamics are shown in figure 5. This figure shows a sequence of images taken from the frozen atomic structures. The simulation of the coalescence of the Au nanoparticles was proposed using two cuboctahedral structures. Figure 5a shows the initial configuration of both cuboctahedral nanoparticles. The presence of twin boundaries in the large cuboctahedral nanoparticle is indicated with arrows. Figure 5b corresponds to the subsequent configuration of the energy minimization configuration state. Figure 5c shows the initial stages of the coalescence phenomenon. Diffusion of atomic superficial species to the neck region can be observed. This situation remains in all the configurations of the

figure 5, and also, this behavior was observed in the experimental in-situ HAADF-STEM images (figures 3 and 4). During the evolution of the coalescence phenomenon, the twin boundaries atomic structure remains and finally there is an atomic planes alignment which gives rise to single crystalline particle. The system energy remains constant during the coalescence process. This is related with a quasi-stable state evolution. The system therefore remains in equilibrium and the last atomic configuration (figure 5i) is the most stable from the energy point of view.

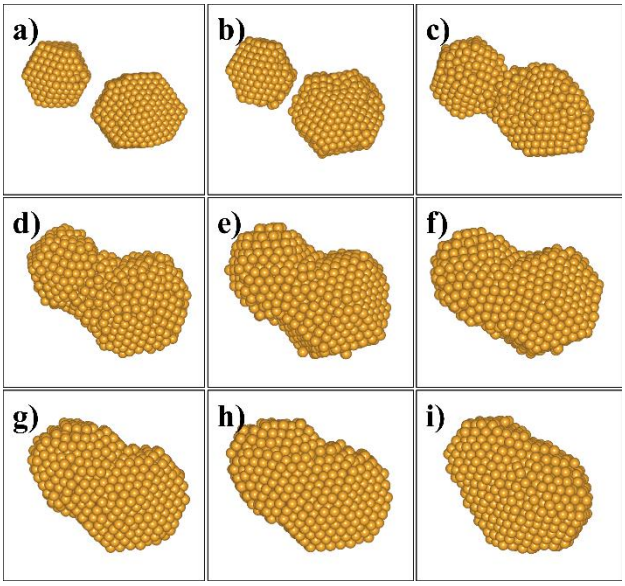

Fig. 5. a) - i) Structure of Au nanoparticles in different stages of the coalescence process.

HAADF-STEM theoretical calculations based on structural models of molecular dynamics of the coalescence evolution were performed. Figure 6 shows the simulated images sequence of the two cuboctahedral nanoparticles, where one of them has two {111} twin boundaries. At different times of the evolution of the coalescence process, the instantaneous atomic positions of the coalescent nanoparticle have been obtained generating the corresponding models which have been used to simulate the STEM images. These theoretical calculations based on the multislice approach of the electron diffraction dynamical theory [21] used the electron microscope parameters illustrated in Table 1. Figure 6a shows the simulated HAADF-STEM image of two Au nanoparticles before the coalescence. The image of the cuboctahedral nanoparticle shows the traces of the twin boundaries. They are indicated with the arrows. Both cuboctahedral nanoparticles are oriented along different zone axis. Figure 6b shows the initial stages of the coalescence phenomenon. The formation of the sintering neck region between the nanoparticles is clearly illustrated. This formation is mainly induced by atomic surface diffusion, as is illustrated in this figure.

Similar to the predicted behavior in the experimental case, the small nanoparticle continues rotating to reach an orientation similar to the other one (figure 6c). Figures 6d and 6e show the two nanoparticles with similar orientation, also, monatomic steps are illustrated in these figures. There is a small rotation, which is more evident for the nanoparticle with the twin boundaries. Figures 6f and 6g show another rotated situation of both nanoparticles, where the image contrast displayed by the twin boundaries tends to disappear. However, figure 6h show another rotation where the twin boundaries can be observed, therefore, the nanoparticle rotates continuously, from a position where the twin's boundaries cannot be observed, forming the coincidence lattice, to another position where the twin's boundaries can be observed. Finally, figure 6i shows the last simulated image, where the tendency to form a single crystalline unit is clearly seen.

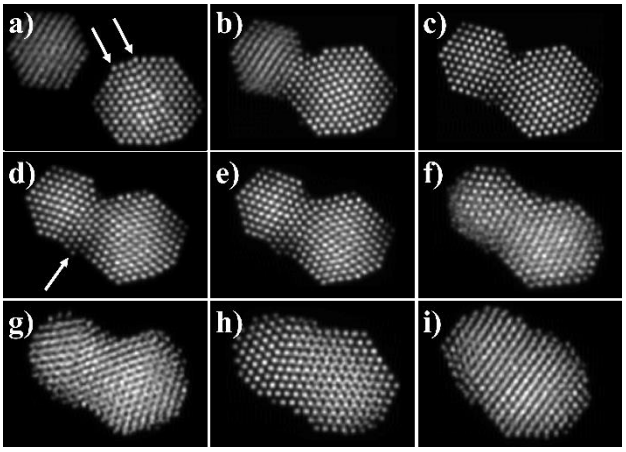

Fig. 6. a) - i) Simulated HAADF-STEM images sequence of the coalescence of the gold nanoparticles.

The STEM images based on the atomic structural models obtained from the molecular dynamical evolution of the coalescence phenomenon can qualitatively reproduce some of the most important characteristics of the experimental in-situ coalescence phenomenon. The rotation of the nanoparticles can clearly be seen from the STEM image contrast and also from the image contrast disappearance of the twin boundaries. Furthermore, the sintering neck formation of the coalescent nanoparticles seems to be induced by the atomic surface diffusion phenomenon.

CONCLUSIONS

Atomic resolution images at 80 kV in STEM mode using spherical aberration corrected were obtained. Some interesting image contrast characteristics were obtained from the sequence HAADF-STEM images. The sintering neck formation is induced by surface diffusion, where the {111} twin boundaries of the nanoparticle act as a barrier to the neck growing mechanism. It is important to point out that the molecular dynamical simulation of the coalescence phenomenon predicts rotations of the nanoparticles. Also, reports in the past have indicated that the electron beam can induce rotations in the nanoparticles. This investigation clearly shows the constant rotation of the coalescence nanoparticles.

REFERENCES

[1] Baletto F. and Ferrando R. (2005) "Structural properties of nanoclusters: Energetic, thermodynamic, and kinetic effects" *Reviews of Modern Physics* 77: 371

[2] Fedlheim D.L. and Foss C.A. (2001) "*Metal nanoparticles: synthesis, characterization, and applications"* CRC press

[3] Mohanraj V. and Chen Y. (2006) "Nanoparticles-a review" *Tropical Journal of Pharmaceutical Research* 5: 561-73

[4] Rodríguez-López J., Montejano-Carrizales J., Palomares-Báez J., Barrón-Escobar H., Velázquez-Salazar J.J., Cabrera-Trujillo J. and José-Yacamán M. 2010 Size effect and shape stability of nanoparticles. In: *Key Engineering Materials*: Trans Tech Publ) pp 47-68

[5] Jensen P. (1999) "Growth of nanostructures by cluster deposition: Experiments and simple models" *Reviews of Modern Physics* 71: 1695

[6] Asoro M., Kovar D., Shao-Horn Y., Allard L. and Ferreira P. (2009) "Coalescence and sintering of Pt nanoparticles: in situ observation by aberration-corrected HAADF STEM" *Nanotechnology* 21: 025701

[7] Gutiérrez-Wing C., Olmos-Asar J.A., Esparza R., Mariscal M. and Yacamán M. (2013) "The role of ad-atoms in the coalescence of alkanethiol-passivated gold nanoparticles" *Electrochimica Acta* 101: 301-7

[8] Antúnez-García J., Mejía-Rosales S., Perez-Tijerina E., Montejano-Carrizales J.M. and José-Yacamán M. (2011) "Coalescence and collisions of gold nanoparticles" *Materials* 4: 368-79

[9] Jose-Yacaman M., Gutierrez-Wing C., Miki M., Yang D.-Q., Piyakis K. and Sacher E. (2005) "Surface diffusion and coalescence of mobile metal nanoparticles" *The Journal of Physical Chemistry B* 109: 9703-11

[10] Hawa T. and Zachariah M.R. (2006) "Coalescence kinetics of unequal sized nanoparticles" *Journal of Aerosol Science* 37: 1-15

[11] Ingham B., Lim T.H., Dotzler C.J., Henning A., Toney M.F. and Tilley R.D. (2011) "How Nanoparticles Coalesce: An in Situ Study of Au Nanoparticle Aggregation and Grain Growth" *Chemistry of Materials* 23: 3312-7

[12] Theissmann R., Fendrich M., Zinetullin R., Guenther G., Schierning G. and Wolf D.E. (2008) "Crystallographic reorientation and nanoparticle coalescence" *Physical Review B* 78: 205413

[13] Egerton R.F., Li P. and Malac M. (2004) "Radiation damage in the TEM and SEM" *Micron* 35: 399-409

[14] Mariscal M.M., Mayoral A., Olmos-Asar J.A., Magen C., Mejía-Rosales S., Pérez-Tijerina E. and José-Yacamán M. (2011) "Nanoalloying in real time. A high resolution STEM and computer simulation study" *Nanoscale* 3: 5013-9

[15] Bell D.C., Russo C.J. and Kolmykov D.V. (2012) "40keV atomic resolution TEM" *Ultramicroscopy* 114: 31-7

[16] Spence J.C. (2013) "*High-resolution electron microscopy"* OUP Oxford

[17] Hawkes P.W. (2004) "*Advances in imaging and electron physics"* Elsevier

[18] Brust M., Walker M., Bethell D., Schiffrin D.J. and Whyman R. (1994) "Synthesis of thiol-derivatised gold nanoparticles in a two-phase Liquid–Liquid system" *Journal of the Chemical Society, Chemical Communications* 801-2

[19] Ishizuka K. (2005) "Deconvolution Processing in Analytical STEM: Monochromator for EELS and Cs-Corrector for STEM-HAADF" *Microscopy and Microanalysis* 11: 1430-1

[20] Koch C. 2002 Determination of core structure periodicity and point defect density along dislocations. Arizona State University Phoenix, AZ)

[21] Cowley J.M. and Moodie A.F. (1957) "The scattering of electrons by atoms and crystals. I. A new theoretical approach" *Acta Crystallographica* 10: 609-19

[22] Li G.J., Wang Q., Zhang Y.J., Cao Y.Z. and He J.C. (2011) "Molecular Dynamics Simulation Study of the Structural Evolution in the Cu-Ni Coalescence Induced by Ni Heterocluster" *Advanced Materials Research* 299-300: 395-8

[23] Shenogin S. and Ozisik R. 2007 Xenoview: visualization for atomistic simulations.

[24] Sasaki T., Sawada H., Hosokawa F., Kohno Y., Tomita T., Kaneyama T., Kondo Y., Kimoto K., Sato Y. and Suenaga K. (2010) "Performance of low-voltage STEM/TEM with delta corrector and cold field emission gun" *Journal of Electron Microscopy* 59: S7-S13

[25] Börrnert F., Bachmatiuk A., Gorantla S., Wolf D., Lubk A., Büchner B. and Rümmeli M.H. (2013) "Retro-fitting an older (S)TEM with two Cs aberration correctors for 80 kV and 60 kV operation" *Journal of microscopy* 249: 87-92

[26] Hofmeister H. (2007) "High-resolution electron microscopy studies of metal nanoparticles: shape and twin defects, and surface stress effects" *Journal of Optoelectronics and Advanced Materials Research* 9: 99

[27] Surrey A., Pohl D., Schultz L. and Rellinghaus B. (2012) "Quantitative Measurement of the Surface Self-Diffusion on Au Nanoparticles by

Aberration-Corrected Transmission Electron Microscopy" *Nano Letters* 12: 6071-7

[28] Chang L.Y., Barnard A.S., Gontard L.C. and Dunin-Borkowski R.E. (2010) "Resolving the Structure of Active Sites on Platinum Catalytic Nanoparticles" *Nano Letters* 10: 3073-6

[29] Potin V., Nouet G., Ruterana P. and Pond R.C. (1999) "The Atomic Structure of Threading Dislocations from Low-Angle to High-Angle Grain Boundaries in GaN/Sapphire Epitaxial Layers" *Physica Status Solidi B* 216: 645-8